RESEARCH ARTICLE

Molecular Docking, Synthesis, Antiproliferative Activity against MCF-7, and *In-vitro* Alpha Amylase Activities of Newer Generation Pyrimidino Hydroxamic Acid Derivatives

Samiya[1], Supriyo Saha[1*], Vikash Jakhmola[1], Nidhi Gairola[1], Mahipal Singh[2]

[1]*Uttaranchal Institute of Pharmaceutical Sciences, Uttaranchal University, Dehradun, Uttarakhand, India.*
[2]*School of Agriculture, Uttaranchal University, Dehradun Uttarakhand India.*

Received: 21st January, 2024; Revised: 12th March, 2024; Accepted: 26th April, 2024; Available Online: 25th June, 2024

ABSTRACT

A set of newer generation pyrimidine hydroxamic acid derivatives were designed, synthesized, and evaluated for antiproliferative activity against breast cancer cell line and *in-vitro* alpha-amylase activity. The design of the molecules was fully dependent upon the structural features of suberoyl anilide hydroxamic acid. Then all the designed molecules (S1-S100) were docked with 4LXZ HDAC2 enzyme and S1, S2, S16 showed good docking interaction scores as compared to SAHA. The interacting residues of (S1, S2, S16) and 4LXZ showed similar amino acid lining as present in the active site. The synthetic procedure of the molecules (S1, S2, S16) was divided into three parts such as synthesis of chalcone derivative using aromatic aldehyde and acetophenone, the reaction between chalcone and thiourea to form substituted pyrimidine-2-thiol, then finally substituted pyrimidine-2-thiol and 2-chloro-N-hydroxyacetamide reacted in the presence of dimethylformamide to obtain the best-docked molecules. All the molecules showed characteristic peaks in fourier-transform infrared (FTIR), proton nuclear magnetic resonance (^{1}H-NMR) and mass spectrometry with sharp melting points and single peak in thin layer chromatography (TLC) plate. Finally antiproliferative activity against MCF-7 and *in-vitro* alpha amylase activity data confirmed that S1 was the best molecule among all the synthesized molecules.

Keywords: Pyrimidine hydroxamic acid, Histone deacetylase, Molecular docking, Synthesis, Antiproliferative activity, *In-vitr*o alpha amylase activity.

International Journal of Drug Delivery Technology (2024); DOI: 10.25258/ijddt.14.2.06

How to cite this article: Samiya, Saha S, Jakhmola V, Gairola N, Singh M. Molecular Docking, Synthesis, Antiproliferative Activity against MCF-7, and *In-vitro* Alpha Amylase Activities of Newer Generation Pyrimidino Hydroxamic Acid Derivatives. International Journal of Drug Delivery Technology. 2024;14(2):649-659.

Source of support: Nil.

Conflict of interest: None

INTRODUCTION

Histone deacetylase (HDAC) enzyme was found to be one of the leading targets for developing anticancer agents.[1] HDAC enzyme was a part of multiprotein complexes, which catalyzed the removal of acetyl group from lysine residue on protein.[2,3] HDAC inhibitors bind with the active site and block substrate access, followed by a resultant accumulation of acetylated histones. (HDACIs) Histone deacetylase inhibitors were responsible to induce inhibition of tumor growth, cell differentiation and apoptosis.[4] Most of the current HDAC inhibitors were pan-caspase inhibitors and bind with the catalytic zinc metal ion in the different HDAC isoforms. Cellular processes depend on HDAC activity. Among the HDAC multiprotein complex (Figure 1),[5] HDAC-8 was selected (due to its *Homo sapiens* source), co-crystallized with ligand (SAHA) suberoyl anilide hydroxamic acid. Ricolinostat a recently developed HDAC inhibitor showed good antidiabetic activity by regulating glucose homeostasis and insulin sensitivity (in clinical trial).[6]

The principal molecule was SAHA. The structure of SAHA consisted of three basic parts as: Surface recognition, linker and metal binding. In this study, the surface recognition group is substituted with the substituted pyrimidine group, linker portion is substituted with the thiomethane group and metal binding portion is a hydroxamic acid group (Figure 2).[7,8]

In this manuscript, we designed, synthesized, perform antiproliferative activities against MCF-7 cell line and *in-vitro* alpha-amylase inhibitors of newer generation pyrimidine hydroxamic acid derivatives.

MATERIALS AND METHODS

All the chemicals were procured from Sigma Aldrich. The progression of the reaction was accessed by precoated Merck thin layer chromatography (TLC) plates using n-hexane and

**Author for Correspondence: supriyo9@gmail.com*

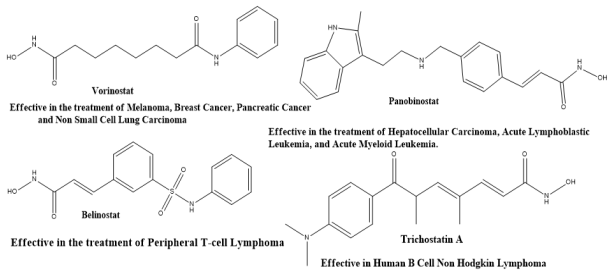

Figure 1: Established HDAC inhibitors

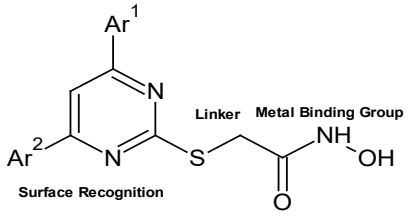

Figure 2: Structure of the proposed hydroxamic acid derivative

ethyl acetate as a solvent system with (9:1) ratio. The melting points of the samples were accessed by EI digital melting point apparatus. The infrared spectrum of synthesized molecules was recorded using a Perkin Elmer fourier transform infrared. (FTIR) spectrophotometer. Proton NMR (^{1}H-NMR) spectra were recorded using Bruker Avance DRX300 300 MHz FTNMR spectrometer using dimethyl sulfoxide. The chemical shifts were measured at δ units (reported as ppm) relative to tetramethylsilane (TMS) and signals are reported as singlet (s), doublet (d), triplet (t), quartet (q), multiplet (m). Mass spectra are also recorded. FTIR, ^{1}H-NMR, and mass spectra were done by the Central Instrumentation Facility of DRI, Uttaranchal University and CDRI, Lucknow. The help of Shimadzu UV-1900i spectroscopy did UV spectroscopy. Elemental analysis was performed using a microanalytical unit.

Molecular Docking Study

Preparation of protein

The protein was modeled by MGL Tools 1.5.6 package (Molecular Graphics Laboratory, the Scripps Research Institute, La Jolla, USA). 4LXZ is the crystal structure of HDAC2 complexed suberoyl anilide hydroxamic acid. The interacting residues of the complexed ligand SAHA were PRO 34, ASP 104, HIS 146, PHE 155, PHE 210, HIS 145, GLY 154, LEU 276, GLY 306, TYR 308 (Figure 3).[9] The receptor contains three chains with amino acids on each chain. At first, all the hetero atoms (water molecules and the co-crystal occupying the substrate binding site) were removed. During the process the deviation in coordinates were rectified by energy minimization using a Swiss PDB viewer (SPDBV 4.1.0, Swiss Institute of Bioinformatics). The energy-minimized protein in pdb format was then subjected to Python Molecular viewer. Later, bond orders were assigned, and polar and missing hydrogens were merged with the inclusion of partial Gasteiger atomic charges. The missing hydrogens and protonation states were by H^{++} server. Finally, in order to make it docking software compatible, all the atoms in the protein were made to Autodock4 type (t) and the pdb file of the protein was converted to pdbqt, where q defines the charge and t for Autodock4 type.

Preparation of ligand molecules

The programme Avogadro was used to create the structures of the designed molecules (S1-S100). MMFF94 force field and steepest descent techniques were used to optimize the molecules. After that, the Open Babel programme was used to add all three-dimensional coordinates to the layout. The molecules were then saved in the PDBQT format after AutoDock Vina was used to add all of the polar hydrogens and gasteiger charges.

Molecular docking parameter

Gasteiger charges were applied to the receptor and ligand molecules, which were then stored in the PDBQT format. The optimal ligand binding site inside each protein was found using the Lamarckian genetic algorithm. The following is a list of the default grid box dimensions for protein-ligand docking. The output of the ligand-protein docking experiments was set to conformations. Lastly, BIOVIA Discovery Studio Visualizer 4.5 were used to visualize and analyse the docking results. The 4LXZ receptor's grid box dimensions were size_x = 24, size_y = 24, size_z = 24, exhaustiveness = 8, and center_x = 21.459, center_y = -20.411, center_z = -3.571.

Validation of molecular docking

Validation is an important step to ensure the reliability and reproducibility of the docking process. It is done by redocking the ligand preoccupying the active site. The active site was emptied by removing the co-crystal, suberoyl anilide hydroxamic acid, from the co-crystallized structure of the protein (PDB: 4LXZ) and thereafter redocked within the active site of the protein. The root mean square deviation (RMSD) between the redocked conformation and the unprocessed crystallographic conformation of compound SHH was found to be <1.0 Å. This ensures the reliability of the docking method in regenerating the experimentally observed binding mode for the receptor.[10]

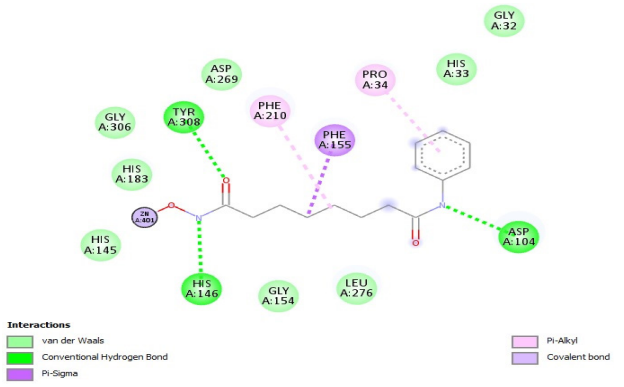

Figure 3: Interacting residues of SAHA within the receptor 4LXZ

Table 1: Structure of the pyrimidine hydroxamic acid derivatives

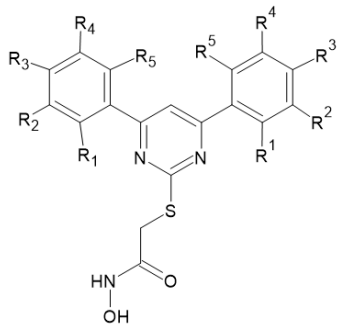

S No	*Sample code*	*R^1*	*R^2*	*R^3*	*R^4*	*R^5*	*R_1*	*R_2*	*R_3*	*R_4*	*R_5*
1	S1	H	H	H	H	H	H	H	H	H	H
2	S2	OH	H	H	H	H	H	H	H	H	H
3	S3	Cl	H	H	H	H	H	H	H	H	H
4	S4	Br	H	H	H	H	H	H	H	H	H
5	S5	OH	H	H	OH	H	H	H	H	H	H
6	S6	H	H	H	OH	H	H	H	H	H	H
7	S7	H	H	H	H	OH	H	H	H	H	H
8	S8	H	H	H	H	H	OH	H	H	H	H
9	S9	H	H	H	H	H	OH	H	H	OH	H
10	S10	H	H	Cl	H	H	H	H	H	H	H
11	S11	H	H	H	H	H	H	H	Cl	H	H
12	S12	H	H	H	Cl	H	H	H	H	H	H
13	S13	Cl	H	H	H	H	Cl	H	H	H	H
14	S14	F	H	H	H	H	H	H	H	H	H
15	S15	H	H	NH_2	H	H	H	H	H	H	H
16	S16	OH	H	H	H	H	H	H	OH	H	H
17	S17	NH_2	H	H	H	H	H	H	H	H	H
18	S18	H	H	NH_2	H	H	H	H	NH_2	H	H
19	S19	NO_2	H	H	H	H	H	H	H	H	H
20	S20	H	H	NO_2	H	H	H	H	NO_2	H	H
21	S21	H	Br	H	H	H	H	H	H	H	H
22	S22	H	Br	H	H	H	H	Br	H	H	H
23	S23	H	Br	H	H	H	H	Cl	H	H	H
24	S24	H	Cl	H	H	H	H	H	H	H	H
25	S25	H	Cl	H	H	H	H	Cl	H	H	H
26	S26	H	Cl	H	H	H	H	Br	H	H	H
27	S27	H	NO_2	H	H	H	NH_2	H	H	H	H
28	S28	H	F	H	H	H	H	Cl	H	H	H
29	S29	H	H	F	H	H	H	Cl	H	H	H
30	S30	H	H	H	OH	H	H	H	H	OH	H
31	S31	H	H	H	Cl	H	H	H	H	OH	H
33	S32	H	H	OCH_3	H	H	H	H	H	OH	H
34	S34	H	H	OCH_3	H	H	H	H	H	H	H
35	S35	H	H	H	H	H	H	H	H	OCH_3	H
36	S36	H	H	OCH_3	OH	H	H	H	H	H	H
37	S37	H	H	OCH_3	OH	H	H	H	OCH_3	OH	H

38	S38	H	H	H	OCH_3	H	H	H	OCH_3	H	H
39	S39	H	H	OCH_3	OH	H	H	H	H	Cl	H
40	S40	H	H	H	NO_2	H	H	H	OCH_3	OH	H
41	S41	H	H	H	NH_2	H	H	H	OCH_3	OH	H
42	S42	H	H	OCH_3	OH	H	H	H	NO_2	H	H
43	S43	H	H	OCH_3	OH	H	H	H	H	NO_2	H
44	S44	H	H	H	OCH_3	OH	H	H	H	NO_2	H
45	S45	H	OCH_3	OH	H	H	H	H	OCH_3	OH	H
46	S46	H	OCH_3	OH	H	H	H	H	H	OCH_3	OH
47	S47	H	OCH_3	OH	H	H	H	OCH_3	OH	H	H
48	S48	H	OCH_3	OH	H	H	H	H	H	H	NO_2
49	S49	OCH_3	OH	H	H	H	H	H	H	H	H
50	S50	OCH_3	OH	H	H	H	OCH_3	OH	H	H	H
51	S51	OCH_3	OH	H	H	H	F	H	H	H	H
52	S52	OCH_3	OH	H	H	H	Br	H	H	H	H
53	S53	OCH_3	OH	H	H	H	Cl	H	H	H	H
54	S54	OCH_3	OH	H	H	H	NH_2	H	H	H	H
55	S55	OCH_3	OH	H	H	H	H	F	H	H	H
56	S56	OCH_3	OH	H	H	H	H	Cl	H	H	H
57	S57	OCH_3	OH	H	H	H	H	Br	H	H	H
58	S58	OCH_3	OH	H	H	H	H	NH_2	H	H	H
59	S59	OCH_3	OH	H	H	H	H	H	F	H	H
60	S60	OCH_3	OH	H	H	H	H	H	Cl	H	H
61	S61	OCH_3	OH	H	H	H	H	H	Br	H	H
62	S62	OCH_3	OH	H	H	H	H	H	NH_2	H	H
63	S63	OCH_3	OH	H	H	H	H	H	H	F	H
64	S64	OCH_3	OH	H	H	H	H	H	H	Br	H
65	S65	OCH_3	OH	H	H	H	H	H	H	Cl	H
66	S67	OCH_3	OH	H	H	H	H	H	H	NH_2	H
67	S67	OCH_3	OH	H	H	H	H	H	H	H	F
68	S68	OCH_3	OH	H	H	H	H	H	H	H	Cl
69	S69	OCH_3	OH	H	H	H	H	H	H	H	Br
70	S70	OCH_3	OH	H	H	H	H	H	H	H	NH_2
71	S71	H	CH_3	OH	H	H	H	H	H	H	H
72	S72	H	CH_3	OH	H	H	H	H	F	H	H
73	S73	H	CH_3	OH	H	H	H	H	Cl	H	H
74	S74	H	CH_3	OH	H	H	H	H	Br	H	H
75	S75	H	CH_3	OH	H	H	H	H	NH_2	H	H
76	S76	H	CH_3	OH	H	H	H	H	H	F	H
77	S77	H	CH_3	OH	H	H	H	H	H	Cl	H
78	S78	H	CH_3	OH	H	H	H	H	H	Br	H
79	S79	H	CH_3	OH	H	H	H	H	H	NH_2	H
80	S80	H	CH_3	OH	H	H	H	H	H	H	F
81	S81	H	CH_3	OH	H	H	H	H	H	H	Cl
82	S82	H	CH_3	OH	H	H	H	H	H	H	Br
83	S83	H	CH_3	OH	H	H	H	H	H	H	NH_2
84	S84	H	H	CH_3	OH	H	H	H	H	H	F

85	S85	H	H	CH_3	OH	H	H	H	H	H	Cl
86	S86	H	H	CH_3	OH	H	H	H	H	H	Br
87	S87	H	H	CH_3	OH	H	H	H	H	H	NH_2
88	S88	H	H	CH_3	OH	H	H	H	H	F	H
89	S89	H	H	CH_3	OH	H	H	H	H	Cl	H
90	S90	H	H	CH_3	OH	H	H	H	H	Br	H
91	S91	H	H	CH_3	OH	H	H	H	H	NH_2	H
92	S92	H	H	H	CH_3	OH	H	F	H	H	H
93	S93	H	H	H	CH_3	OH	H	Cl	H	H	H
94	S94	H	H	H	CH_3	OH	H	Br	H	H	H
95	S95	H	H	H	CH_3	OH	H	NH_2	H	H	H
96	S96	H	H	H	CF_3	OH	H	H	H	H	H
97	S97	H	H	H	CF_3	OH	H	F	H	H	H
98	S98	H	H	H	CF_3	OH	H	Cl	H	H	H
99	S99	H	H	H	CF_3	OH	H	Br	H	H	H
100	S100	H	H	H	CF_3	OH	H	NH_2	H	H	H

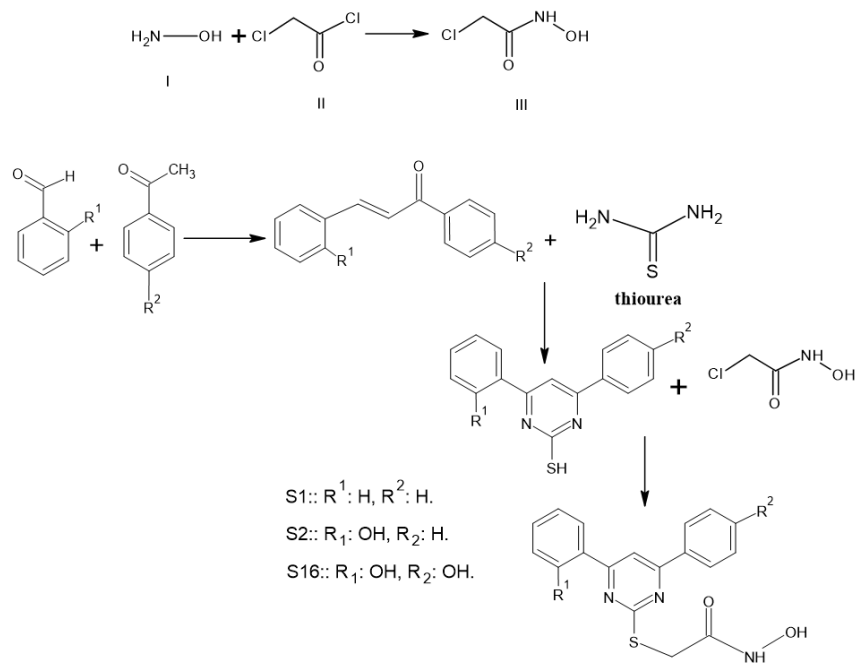

Figure 4: Synthetic procedures of S1, S2 and S16

Synthesis

Based on the docking score of the designed molecules (S1-S100), we synthesized the top 3 molecules S1, S2 and S16. Table 1 shows all the structures of the designed pyrimidine hydroxamic acid derivatives.[11]

Synthesis of 2-chloro-N-hydroxyacetamide (III)

Methanol (12 mL) and 0.0336 M, 2.34 g of hydroxylamine hydrochloride (I) were placed over a heated magnetic plate in a flask. The mixture was stirred for 5 minutes and added dropwise to a previously prepared methanol solution of 0.0501 M, 2.81 g potassium hydroxide. Then, the resulting solution was cooled to room temperature and filtered. The filtrate was stored and used for the next step. Then 25 mL of methanol was taken in a 250 mL beaker and stirred over a magnetic stirrer. The total synthetic setup was done under the fuming cupboard. Poured 0.07 M, 5.6 mL of chloroacetyl chloride (II) from the dropping funnel into the methanol and was mixed it properly. Choloroacetyl chloride and hydroxylamine solutions were stirred for 2 hours. The product was obtained by filtration. Filtrate was washed with diethyl ether and recrystallized from methanol.[12]

Synthesis of 2-[(4,6-diphenylpyrimidin-2-yl)sulfanyl]-N-hydroxyacetamide (S1)

In the first step, benzaldehyde and acetophenone reacted in the presence of methanol to produce (2E)-1,3-diphenylprop-2-en-1-one followed by a reaction with thiourea to obtain 4,6-diphenylpyrimidine-2-thiol. Finally, 4,6-diphenylpyrimidine-2-thiol and 2-chloro-N-hydroxyacetamide in the presence of dimethylformamide to get 2-[(4,6-diphenylpyrimidin-2-yl)sulfanyl]-N-hydroxyacetamide.

Synthesis of N-hydroxy-2-{[4-(2-hydroxyphenyl)-6-phenylpyrimidin-2-yl]sulfanyl}acetamide (S2)

In the first step, 2-hydroxybenzaldehyde and acetophenone reacted in the presence of methanol to produce (2E)-1,3-diphenylprop-2-en-1-one followed by a reaction with thiourea to obtain 4,6-diphenylpyrimidine-2-thiol. Finally 4,6-diphenylpyrimidine-2-thiol and 2-chloro-N-hydroxyacetamide in presence of dimethylformamide to get N-hydroxy-2-{[4-(2-hydroxyphenyl)-6-phenylpyrimidin-2-yl] sulfanyl}acetamide.

Synthesis of N-hydroxy-2-{[4-(2-hydroxyphenyl)-6-(4-hydroxyphenyl)pyrimidin-2-yl]sulfanyl}acetamide (S16)

In the first step, 2-hydroxybenzaldehyde and 4-hydroxyacetophenone reacted in presence of methanol to produce (2E)-1,3-diphenylprop-2-en-1-one followed by reaction with thiourea to obtain 4,6-diphenylpyrimidine-2-thiol. Finally 4,6-diphenylpyrimidine-2-thiol and 2-chloro-N-hydroxyacetamide in presence of dimethylformamide to get N-hydroxy-2-{[4-(2-hydroxyphenyl)-6-(4-hydroxyphenyl) pyrimidin-2-yl]sulfanyl}acetamide (Figure 4).[13]

Antiproliferative Assay of Synthesized Molecules on MCF-7

The antiproliferative activity of the synthesized molecules against MCF-7 breast cancer cell line was assessed using the sulphorodamine B assay. Initially, the culture was set using trichloroacetic acid followed by staining using 0.4% (w/v) sulforhodamine B. Then protein-linked dye was extracted using 10 mM unbuffered tris base [tris hydroxymethyl) aminomethane] in order to determine optical density. Protein unbound dye was washed with 1% acetic acid solution. The SRB assay was performed based on Lowry and Bradford test procedures. The signal to noise ratio at 564 nm was 1.5 with 1000 cells. This approach showed high valued automated drug screening process to quantify cell toxicity. SRB fluorescence with laser illumination at 488 nm was measured using static fluorescence cytometry.[14]

***In-vitro* Alpha Amylase Inhibition Assay**

Stock solutions of synthesized molecules were prepared in two phases, in the first step 100 mg of drug sample was dissolved in 1-mL DMSO, followed by diluting upto 100 mL in methanol. Then prepared 10, 20, 30, 40, 60 µg/mL solutions using methanol as diluents. Standard acarbose solution was prepared in water followed by its consecutive dilutions in the same solvent. In a 96-well plate reaction mixture 50 µL 100 mM, pH = 6.8 phosphate buffer, 10 µL 2 unit/mL α–amylase, and 20 µL of synthesized molecules or standard acarbose were incubated at 37°C temperature for 20 minutes. Then 20 µL of 1% soluble starch (prepared in 100 mM phosphate buffer pH 6.8) was added and incubated at 37°C temperature for 30 minutes. Further, 100 µL of the dinitrosalicylic acid was added and boil for 10 minutes. The absorbance of the resulting mixture was taken at 540 nm using UV-visible spectroscopy (UV-1900i). Acarbose at various concentrations was considered as standard. Control was considered as a reagent without a sample solution and every experiment was performed in a triplicate manner.[15]

RESULTS AND DISCUSSION

Molecular Docking Study

The molecular docking studies of the designed pyrimidine hydroxamic acid derivatives (S1-S100) with 4LXZ receptor showed docking scores ranging from -5.2 kcal/mol to -7.4 kcal/mol whereas standard SAHA showed docking score of -7.4 kcal/mol. All the synthesized molecules effectively bound within the receptor active site and shared similar amino acid residues as complexed ligands. S1, S2 and S16 showed good docking interaction scores of -7.4, -7.4, and -7.3 kcal/mol, respectively. The molecule S1 interacted with ASP 104 by hydrogen bond interaction and PHE 155, HIS 183, PHE 210, TYR 209 by pi-pi interactions. S2 interacted with GLU 208, PHE 210 by hydrogen bond interaction, and PHE 155, HIS 183 by pi-pi interactions. S16 interacted with ASP 104, GLU 208 by hydrogen bond interactions; PHE 155, HIS 183, TYR 209, PHE 210 by pi-pi interactions; and PRO 34 by Van der Waal interaction. These below-mentioned amino acid residues are similar between synthesized molecules and complexed ligand: S1: ASP 104, PHE 155, PHE 210; S2: PHE 210, PHE 155; S16: ASP 104, PHE 155, PHE 210, and PRO 34 (Figure 5 and Table 2).[16,17]

Synthesis

Melting point, FTIR, ^{1}H-NMR, mass spectrometry and elemental analysis characterized all the synthesized molecules. The synthesized molecules showed single peak during chromatographic assessments.

S1

Yield = 35.45%, MP= 145ºC. FTIR (KBr) v/cm^{-1}: 3319 (OH str), 3650 (NH str), 1777 (C=O str), 2926 (C=S str), 1897–1970 (Aromatic ring str). ^{1}H-NMR DMSO (300 MHz) δ ppm: 2.72 (-CH_2- str), 8.07 (NH str), 10.3 (OH str), 7.11 (=CH- str), (7.3–8.3) Ar-H str. $C_{18}H_{15}N_3O_2S$: calculated C: 64.09%, H: 4.45%, N: 12.46%, O: 9.49%. $C_{18}H_{15}N_3O_2S$: calculated C: 63.98%, H: 4.12%, N: 12.32%, O: 9.35%. (M+1): 337.50 (EIMS).

S2

Yield = 42.48%, Mp = 135ºC. FTIR (KBr) v/cm^{-1}: 3212 (OH str), 3726 (NH str), 1781 (C=O str), 2940 (C=S str), 1814–2044 (Aromatic ring str). ^{1}H-NMR DMSO (300 MHz) δ ppm: 2.50 (-CH_2- str), 8.10 (NH str), 10.3 (OH str), 7.25 (=CH- str), (7.34–7.99) Ar-H str. $C_{18}H_{15}N_3O_3S$: calculated C: 61.18%, H: 4.24%,

Table 2: Molecular docking interaction data between of S1-S100 and standard SAHA molecule

S No	*Code of the Molecules*	*Receptor used*	*Dock Score (kcal/mol)*	*Interacting residues*
1.	S1	4LXZ	-7.4	ASP 104a, PHE 155b, HIS 183b, PHE 210b, TYR 209b
2.	S2	4LXZ	-7.4	GLU 208a, PHE 210a, PHE 155b, HIS 183b
3.	S3	4LXZ	-6.8	ASP 104a, GLU 208a, PHE 155b, HIS 183b, TYR 209b, PHE 210b, PRO 34c.
4.	S4	4LXZ	-7.0	LEU 276a, PHE 155b, PHE 210b, ASP 104c, HIS 183d.
5.	S5	4LXZ	-7.0	ASP 104a, PHE 155b, HIS 183b, TYR 209b, PHE 210b.
6.	S6	4LXZ	-6.8	ASP 104a, GLU 208a,GLY 154c, PHE 155b, HIS 183b, TYR 209b, PHE 210b.
7.	S7	4LXZ	-6.9	LEU 276a, PHE 155b, PHE 210b, ASP 104d, HIS 183d, HIS 145c, HIS 146c, TYR 209c, ASP 269c, GLY 306c.
8.	S8	4LXZ	-7.0	HIS 145a, HIS 146b, ASP 181a, HIS183a, PHE 155b, PHE 210b, LEU 276b.
9.	S9	4LXZ	-6.7	ASP 104a, PHE 155b, HIS 183b, PHE 210b, TYR 209b
10.	S10	4LXZ	-6.8	GLU 208a, PHE 210a, PHE 155b, HIS 183b
11.	S11	4LXZ	-6.6	HIS 145a, HIS 146b, ASP 181a, HIS183a, PHE 155b, PHE 210b, LEU 276b.
12.	S12	4LXZ	-6.1	LEU 276a, PHE 155b, PHE 210b, ASP 104d, HIS 183d, HIS 145c, HIS 146c, .TYR 209c, ASP 269c, GLY 306c.
13.	S13	4LXZ	-6.0	ASP 104a, PHE 155b, HIS 183b, PHE 210b, TYR 209b
14.	S14	4LXZ	-6.2	GLU 208a, PHE 210a, PHE 155b, HIS 183b
15.	S15	4LXZ	-6.9	ASP 104a, PHE 155b, HIS 183b, TYR 209b, PHE 210b.
16.	S16	4LXZ	-7.3	ASP 104a, GLU 208a, PHE 155b, HIS 183b, TYR 209b, PHE 210b, PRO 34c
17.	S17	4LXZ	-7.0	LEU 276a, PHE 155b, PHE 210b, ASP 104d, HIS 183d, HIS 145c, HIS 146c, TYR 209c, ASP 269c, GLY 306c.
18	S18	4LXZ	-7.0	HIS 145a, HIS 146b, ASP 181a, HIS183a, PHE 155b, PHE 210b, LEU 276b.
19.	S19	4LXZ	-7.1	ASP 104a, PHE 155b, HIS 183b, TYR 209b, PHE 210b.
20.	S20	4LXZ	-6.4	ASP 104a, PHE 155b, HIS 183b, PHE 210b, TYR 209b
21.	S21	4LXZ	-6.2	GLU 208a, PHE 210a, PHE 155b, HIS 183b
22.	S22	4LXZ	-6.2	ASP 104a, PHE 155b, HIS 183b, TYR 209b, PHE 210b.
23.	S23	4LXZ	-6.1	ASP 104a, PHE 155b, HIS 183b, PHE 210b, TYR 209b
24.	S24	4LXZ	-6.8	GLU 208a, PHE 210a, PHE 155b, HIS 183b
25.	S25	4LXZ	-5.9	ASP 104a, PHE 155b, HIS 183b, TYR 209b, PHE 210b.
26.	S26	4LXZ	-6.0	LEU 276a, PHE 155b, PHE 210b, ASP 104d, HIS 183d, HIS 145c, HIS 146c, TYR 209c, ASP 269c, GLY 306c.
27.	S27	4LXZ	-6.2	HIS 145a, HIS 146b, ASP 181a, HIS183a, PHE 155b, PHE 210b, LEU 276b.
28.	S28	4LXZ	-6.1	ASP 104a, PHE 155b, HIS 183b, TYR 209b, PHE 210b.
29.	S29	4LXZ	-6.2	LEU 276a, PHE 155b, PHE 210b, ASP 104d, HIS 183d, HIS 145c, HIS 146c, TYR 209c, ASP 269c, GLY 306c.
30.	S30	4LXZ	-6.3	HIS 145a, HIS 146b, ASP 181a, HIS183a, PHE 155b, PHE 210b, LEU 276b.
31.	S31	4LXZ	-6.5	ASP 104a, PHE 155b, HIS 183b, PHE 210b, TYR 209b
32.	S32	4LXZ	-6.2	GLU 208a, PHE 210a, PHE 155b, HIS 183b
33.	S33	4LXZ	-6.4	LEU 276a, PHE 155b, PHE 210b, ASP 104d, HIS 183d, HIS 145c, HIS 146c, TYR 209c, ASP 269c, GLY 306c.
34.	S34	4LXZ	-6.6	HIS 145a, HIS 146b, ASP 181a, HIS183a, PHE 155b, PHE 210b, LEU 276b.
35.	S35	4LXZ	-6.1	ASP 104a, PHE 155b, HIS 183b, TYR 209b, PHE 210b.
36.	S36	4LXZ	-5.9	LEU 276a, PHE 155b, PHE 210b, ASP 104d, HIS 183d, HIS 145c, HIS 146c, TYR 209c, ASP 269c, GLY 306c.

37.	S37	4LXZ	-6.2	HIS 145a, HIS 146b, ASP 181a, HIS183a, PHE 155b, PHE 210b, LEU 276b.
38.	S38	4LXZ	-6.4	ASP 104a, PHE 155b, HIS 183b, TYR 209b, PHE 210b.
39.	S39	4LXZ	-6.8	LEU 276a, PHE 155b, PHE 210b, ASP 104d, HIS 183d, HIS 145c, HIS 146c, TYR 209c, ASP 269c, GLY 306c.
40.	S40	4LXZ	-5.9	HIS 145a, HIS 146b, ASP 181a, HIS183a, PHE 155b, PHE 210b, LEU 276b.
41.	S41	4LXZ	-5.9	ASP 104a, PHE 155b, HIS 183b, TYR 209b, PHE 210b.
42.	S42	4LXZ	-6.0	LEU 276a, PHE 155b, PHE 210b, ASP 104d, HIS 183d, HIS 145c, HIS 146c, TYR 209c, ASP 269c, GLY 306c.
43.	S43	4LXZ	-6.1	HIS 145a, HIS 146b, ASP 181a, HIS183a, PHE 155b, PHE 210b, LEU 276b.
44	S44	4LXZ	-6.6	ASP 104a, PHE 155b, HIS 183b, TYR 209b, PHE 210b.
45.	S45	4LXZ	-6.7	LEU 276a, PHE 155b, PHE 210b, ASP 104d, HIS 183d, HIS 145c, HIS 146c, TYR 209c, ASP 269c, GLY 306c.
46.	S46	4LXZ	-6.9	HIS 145a, HIS 146b, ASP 181a, HIS183a, PHE 155b, PHE 210b, LEU 276b.
47.	S47	4LXZ	-7.0	ASP 104a, PHE 155b, HIS 183b, TYR 209b, PHE 210b.
48.	S48	4LXZ	-6.8	LEU 276a, PHE 155b, PHE 210b, ASP 104d, HIS 183d, HIS 145c, HIS 146c, TYR 209c, ASP 269c, GLY 306c.
49.	S49	4LXZ	-6.9	HIS 145a, HIS 146b, ASP 181a, HIS183a, PHE 155b, PHE 210b, LEU 276b.
50.	S50	4LXZ	-6.2	ASP 104a, PHE 155b, HIS 183b, TYR 209b, PHE 210b.
51.	S51	4LXZ	-6.2	LEU 276a, PHE 155b, PHE 210b, ASP 104d, HIS 183d, HIS 145c, HIS 146c, TYR 209c, ASP 269c, GLY 306c.
52.	S52	4LXZ	-6.3	HIS 145a, HIS 146b, ASP 181a, HIS183a, PHE 155b, PHE 210b, LEU 276b.
53	S53	4LXZ	-6.5	ASP 104a, PHE 155b, HIS 183b, TYR 209b, PHE 210b.
54.	S54	4LXZ	-6.8	LEU 276a, PHE 155b, PHE 210b, ASP 104d, HIS 183d, HIS 145c, HIS 146c, TYR 209c, ASP 269c, GLY 306c.
55.	S55	4LXZ	-6.5	HIS 145a, HIS 146b, ASP 181a, HIS183a, PHE 155b, PHE 210b, LEU 276b.
56.	S56	4LXZ	-6.7	GLU 208a, PHE 210a, PHE 155b, HIS 183b
57	S57	4LXZ	-6.9	ASP 104a, PHE 155b, HIS 183b, TYR 209b, PHE 210b.
58.	S58	4LXZ	-6.4	ASP 104a, GLU 208a, PHE 155b, HIS 183b, TYR 209b, PHE 210b, PRO 34c
59.	S59	4LXZ	-6.6	LEU 276a, PHE 155b, PHE 210b, ASP 104d, HIS 183d, HIS 145c, HIS 146c, TYR 209c, ASP 269c, GLY 306c.
60	S60	4LXZ	-6.7	HIS 145a, HIS 146b, ASP 181a, HIS183a, PHE 155b, PHE 210b, LEU 276b.
61.	S61	4LXZ	-6.8	ASP 104a, PHE 155b, HIS 183b, TYR 209b, PHE 210b.
62.	S62	4LXZ	-6.8	ASP 104a, PHE 155b, HIS 183b, PHE .210b, TYR 209b
63.	S63	4LXZ	-5.5	GLU 208a, PHE 210a, PHE 155b, HIS 183b
64.	S64	4LXZ	-5.4	ASP 104a, PHE 155b, HIS 183b, TYR 209b, PHE 210b.
65.	S65	4LXZ	-5.8	ASP 104a, PHE 155b, HIS 183b, PHE 210b, TYR 209b
66.	S66	4LXZ	-5.4	GLU 208a, PHE 210a, PHE 155b, HIS 183b
67.	S67	4LXZ	-5.2	ASP 104a, PHE 155b, HIS 183b, TYR 209b, PHE 210b.
68.	S68	4LXZ	-5.7	LEU 276a, PHE 155b, PHE 210b, ASP 104d, HIS 183d, HIS 145c, HIS 146c, TYR 209c, ASP 269c, GLY 306c.
69.	S69	4LXZ	-5.9	HIS 145a, HIS 146b, ASP 181a, HIS183a, PHE 155b, PHE 210b, LEU 276b.
70.	S70	4LXZ	-6.1	ASP 104a, PHE 155b, HIS 183b, TYR 209b, PHE 210b.
71.	S71	4LXZ	-6.2	LEU 276a, PHE 155b, PHE 210b, ASP 104d, HIS 183d, HIS 145c, HIS 146c, TYR 209c, ASP 269c, GLY 306c.
72.	S72	4LXZ	-6.4	HIS 145a, HIS 146b, ASP 181a, HIS183a, PHE 155b, PHE 210b, LEU 276b.
73.	S73	4LXZ	-6.7	ASP 104a, PHE 155b, HIS 183b, PHE 210b, TYR 209b

74.	S74	4LXZ	-6.5	GLU 208a, PHE 210a, PHE 155b, HIS 183b
75.	S75	4LXZ	-6.6	LEU 276a, PHE 155b, PHE 210b, ASP 104d, HIS 183d, HIS 145c, HIS 146c, TYR 209c, ASP 269c, GLY 306c.
76.	S76	4LXZ	-6.7	HIS 145a, HIS 146b, ASP 181a, HIS183a, PHE 155b, PHE 210b, LEU 276b.
77.	S77	4LXZ	-6.5	ASP 104a, PHE 155b, HIS 183b, TYR 209b, PHE 210b.
78.	S78	4LXZ	-6.6	LEU 276a, PHE 155b, PHE 210b, ASP 104d, HIS 183d, HIS 145c, HIS 146c, TYR 209c, ASP 269c, GLY 306c.
79.	S79	4LXZ	-6.7	HIS 145a, HIS 146b, ASP 181a, HIS183a, PHE 155b, PHE 210b, LEU 276b.
80.	S80	4LXZ	-5.4	ASP 104a, PHE 155b, HIS 183b, TYR 209b, PHE 210b.
81.	S81	4LXZ	-5.6	LEU 276a, PHE 155b, PHE 210b, ASP 104d, HIS 183d, HIS 145c, HIS 146c, TYR 209c, ASP 269c, GLY 306c.
82.	S82	4LXZ	-5.9	HIS 145a, HIS 146b, ASP 181a, HIS183a, PHE 155b, PHE 210b, LEU 276b.
83.	S83	4LXZ	-6.4	ASP 104a, PHE 155b, HIS 183b, TYR 209b, PHE 210b.
84.	S84	4LXZ	-6.2	LEU 276a, PHE 155b, PHE 210b, ASP 104d, HIS 183d, HIS 145c, HIS 146c, TYR 209c, ASP 269c, GLY 306c.
85.	S85	4LXZ	-6.2	GLU 208a, PHE 210a, PHE 155b, HIS 183b
86.	S86	4LXZ	-6.6	ASP 104a, PHE 155b, HIS 183b, TYR 209b, PHE 210b.
87.	S87	4LXZ	-6.2	ASP 104a, GLU 208a, PHE 155b, HIS 183b, TYR 209b, PHE 210b, PRO 34c
88.	S88	4LXZ	-5.9	LEU 276a, PHE 155b, PHE 210b, ASP 104d, HIS 183d, HIS 145c, HIS 146c, TYR 209c, ASP 269c, GLY 306c.
89.	S89	4LXZ	-6.7	HIS 145a, HIS 146b, ASP 181a, HIS183a, PHE 155b, PHE 210b, LEU 276b.
90.	S90	4LXZ	-6.8	ASP 104a, PHE 155b, HIS 183b, TYR 209b, PHE 210b.
91.	S91	4LXZ	-6.7	ASP 104a, PHE 155b, HIS 183b, PHE 210b, TYR 209b
92.	S92	4LXZ	-6.1	GLU 208a, PHE 210a, PHE 155b, HIS 183b
93.	S93	4LXZ	-6.8	ASP 104a, PHE 155b, HIS 183b, TYR 209b, PHE 210b.
94.	S94	4LXZ	-6.4	ASP 104a, PHE 155b, HIS 183b, PHE 210b, TYR 209b
95.	S95	4LXZ	-6.2	GLU 208a, PHE 210a, PHE 155b, HIS 183b
96.	S96	4LXZ	-6.4	ASP 104a, PHE 155b, HIS 183b, TYR 209b, PHE 210b.
97.	S97	4LXZ	-6.7	LEU 276a, PHE 155b, PHE 210b, ASP 104d, HIS 183d, HIS 145c, HIS 146c, TYR 209c, ASP 269c, GLY 306c.
98	S98	4LXZ	-6.6	HIS 145a, HIS 146b, ASP 181a, HIS183a, PHE 155b, PHE 210b, LEU 276b.
99.	S99	4LXZ	-6.2	ASP 104a, PHE 155b, HIS 183b, TYR 209b.
100.	S100	4LXZ	-6.0	ASP 104a, PHE 155b, HIS 183b, TYR 209b, PHE 210b.
101.	SAHA	4LXZ	-7.4	LEU 276a, PHE 155b, PHE 210b, ASP 104d, HIS 183d, HIS 145c, HIS 146c, TYR 209c, ASP 269c, GLY 306c.

a: Hydrogen bond; b: pi-pi interactions; c: van der waal interaction; d: pi-cation/anion interaction

Table 3: Antiproliferative activity data of synthesized molecules on MCF-7

S No	*Code of the molecules*	*LC_{50}*	*TGI*	*GI_{50}*
1.	S1	>80	>80	10.7
2.	S2	>80	>80	17.4
3.	S16	>80	>80	21.4
4.	Adriamycin	58.8	18.6	-50.2

N: 11.89%, O: 13.59%. $C_{18}H_{15}N_3O_3S$: calculated C: 60.82%, H: 4.08%, N: 10.84%, O: 12.94%. (M+1): 353.39 (EIMS).

S16

Yield = 29.35%, Mp = 128ºC. FTIR (KBr) v/cm^{-1}: 3200 (OH str), 3525 (NH str), 1755 (C=O str), 2948 (C=S str), 1806–2020 (Aromatic ring str). ^{1}H-NMR DMSO (300 MHz) δ ppm: 6.68 (-CH_2- str), 9.07 (NH str), 9.81 (OH str), 7.13 (=CH- str), (7.24–7.94) Ar-H str, 8.15 ppm (OH of 4-hydroxybenzene). $C_{18}H_{15}N_3O_4S$: calculated C: 58.53%, H: 4.06%, N: 11.38%, O: 17.34%. $C_{18}H_{15}N_3O_4S$: calculated C: 57.942%, H: 3.88%, N: 10.87%, O: 16.91%. (M+1): 369.39 (EIMS).

All the spectroscopic characterization data confirmed the formation of the designed molecules.[18]

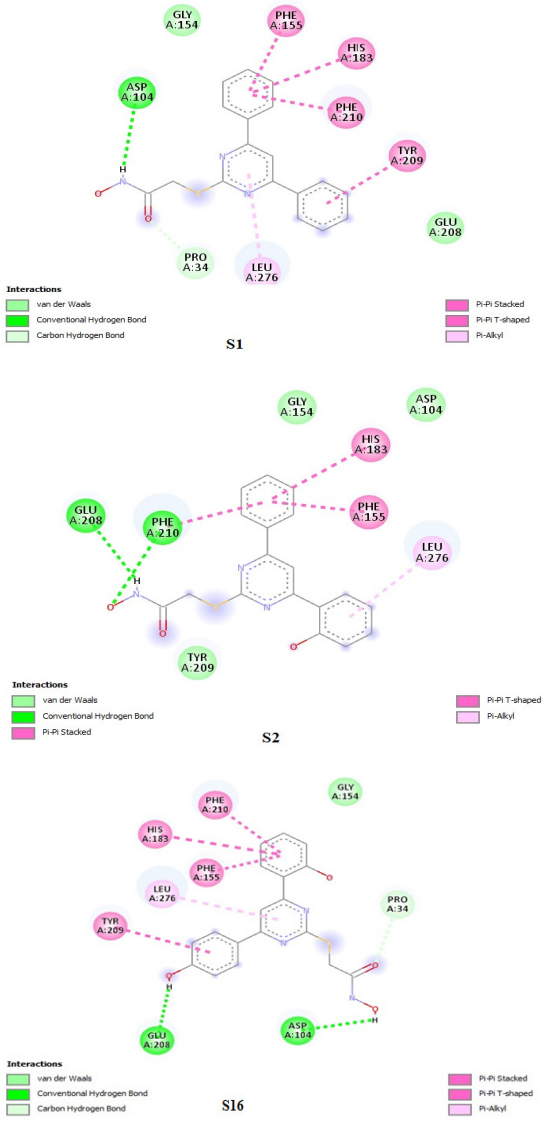

Figure 5: Molecular docking interaction between Synthesized Molecules (S1, S2, S16) with 4LXZ receptor

Antiproliferative Assay Analysis Data of Synthesized Molecules on MCF-7

In this experiment, (LC_{50}) concentration of drug causing 50% cell kill, (TGI) concentration of drug causing total inhibition of cell growth and (GI_{50}) concentration of drug causing 50% inhibition of cell growth were calculated considering adriamycin as positive control. Activity of the synthesized molecules S1, S2, and S16 against MCF-7 cell line reported in Table 3. S1, S2, and S16 showed GI_{50} values of 10.7, 17.4, and 21.4 µM. Standard molecule adriamycin was found with GI_{50} values of (-) 50.2. Among the synthesized molecules, S1 showed a good GI_{50} value as comparison to control.[19]

In-vitro Alpha Amylase Inhibition Assay

The IC_{50} values of all the synthesized molecules (S1, S2, S16) as per *in-vitro* alpha amylase inhibition assay were 10.62, 12.00, and 31.43 µg/mL, respectively, whereas the IC_{50} value of standard acarbose was 66.65 µg/mL. These data were obtained after three consecutive experiments to minimize the error.[18] Among all the synthesized molecules, S1 showed best activity. The activity profile of the molecule was S1>S2> S16 (Table 4).[20, 21]

Table 4: *In-vitro* alpha amylase inhibition assay of synthesized molecules S1, S2, S16 and acarbose

S No.	*Code of the molecules*	*Concentration (µg/mL)*	*%Alpha amylase inhibition*	IC_{50}
1.	S1	10	47.05	10.62
		20	55.39	
		30	61.27	
		40	66.66	
		60	75	
2.	S2	10	41.66	12.00
		20	58.33	
		30	65.68	
		40	71.07	
		60	81.37	
3.	S16	10	21.58	31.43
		20	38.39	
		30	47.72	
		40	71.07	
		60	84.76	
4.	Acarbose	10	5.88	66.65
		20	9.8	
		30	17.64	
		40	30.39	
		50	40.68	
		60	45.09	
		70	52.45	
		80	58.88	

CONCLUSION

The development of newer generation pyrimidino hydroxamic acid derivatives were successfully designed, synthesized, chemically characterized and biologically evaluated as antiproliferative activity against breast cancer cell line and *in-vitro* alpha-amylase inhibitor. Molecular docking studies of the designed (S1-S100) molecules against HDAC2 receptor showed that S1, S2 S16 observed with good docking scores as compared to standard SAHA. Synthesis of the molecules was carried out using simple synthetic procedures and characterized by different spectroscopic methods. Finally antiproliferative activity against MCF-7 and *in-vitro* alpha amylase activity data confirmed that S1 was the best molecule among all the synthesized molecules. So if we established these molecules by *in-vivo* models, then it will be a boon for the mankind.

ACKNOWLEDGMENT

This research is supported by the Division of Research & Innovation, Uttaranchal University, Dehradun, India, under the seed money grant reference no UU/DRI/SM/2023-24/007.

REFERENCES

1. Pal D, Saha S. Hydroxamic acid - A novel molecule for anticancer therapy. Journal of Advanced Pharmaceutical Technology & Research. 2012;3(2):92-9. Available from: doi.org/10.4103/2231-4040.97281
2. Kelly WK, Marks PA. Drug insight: Histone deacetylase inhibitors--development of the new targeted anticancer agent suberoylanilide hydroxamic acid. Nature Reviews Clinical Oncology. 2005;2(3):150-7. Available from: doi.org/10.1038/ncponc0106
3. Ramaiah MJ, Tangutur AD, Manyam RR. Epigenetic modulation and understanding of HDAC inhibitors in cancer therapy. Life Sciences. 2021; 277: 119504. Available from: doi.org/10.1016/j.lfs.2021.119504
4. Bondarev AD, Attwood MM, Jonsson J, Chubarev VN, Tarasov VV, Schiöth HB. Recent developments of HDAC inhibitors: Emerging indications and novel molecules. British Journal of Clinical Pharmacology. 2021; 87(12): 4577-4597. Available from: doi.org/10.1111/bcp.14889
5. Shanmugam G, Rakshit S, Sarkar K. HDAC inhibitors: Targets for tumor therapy, immune modulation and lung diseases. Translational Oncology. 2022;16:101312. Available from: doi.org/10.1016/j.tranon.2021.101312
6. Zeleke TZ, Pan Q, Chiuzan C, Onishi M, Li Y, Tan H, Alvarez MJ, Honan E, Yang M, Chia PL, Mukhopadhyay P, Kelly S, Wu R, Fenn K, Trivedi MS, Accordino M, Crew KD, Hershman DL, Maurer M, Jones S, High A, Peng J, Califano A, Kalinsky K, Yu J, Silva J. Network-based assessment of HDAC6 activity predicts preclinical and clinical responses to the HDAC6 inhibitor ricolinostat in breast cancer. Nature Cancer. 2023;4(2):257-275. Available from: doi.org/10.1038/s43018-022-00489-5.
7. Akter S, Alhatlani BY, Abdallah EM, Saha S, Ferdous J, Hossain ME, Ali F, Kawsar SMA. Exploring Cinnamoyl-Substituted Mannopyranosides: Synthesis, Evaluation of Antimicrobial Properties, and Molecular Docking Studies Targeting H5N1 Influenza A Virus. Molecules. 2023; 28(24): 8001. Available from: doi.org/10.3390/molecules28248001
8. Lokhande KB, Tiwari A, Gaikwad S, Kore S, Nawani N, Wani M, Swamy KV, Pawar SV. Computational docking investigation of phytocompounds from bergamot essential oil against Serratia marcescens protease and FabI: Alternative pharmacological strategy. Computational Biology and Chemistry. 2023; 104: 107829. Available from: doi.org/10.1016/j.compbiolchem.2023.107829
9. Nagare S, Lokhande KB, Swamy KV. Molecular Docking and Simulation Studies of Flavanone and its Derived Compounds on PI3K-AKT Pathway Targeting against Cancer. Current Drug Discovery Technologies. 2023;20(1):e260522205302. Available from: doi.org/10.2174/1570163819666220526150152
10. Saha S, Pal D, Kumar S. Design, synthesis and antiproliferative activity of hydroxyacetamide derivatives against HeLa cervical carcinoma cell and breast cancer cell line. Tropical Journal of Pharmaceutical Research, 2016; 15(7): 1401-1411. Available from: doi.org/10.4314/tjpr.v15i7.8
11. Gilles C, Astier JP, Marchis-Mouren G, Cambillau C, Payan F. Crystal structure of pig pancreatic alpha-amylase isoenzyme II, in complex with the carbohydrate inhibitor acarbose. European Journal of Biochemistry. 1996;238(2):561-9. Available from: doi.org/10.1111/j.1432-1033.1996.0561z.x
12. Gross TD, Zhu YF, Saunders J, Wilcoxen KM, Gao Y, Connors PJ Jr, Guo Z, Struthers RS, Reinhart GJ, Chen C. Design, synthesis and structure-activity relationships of novel imidazolo[1,2-a] pyrimid-5-ones as potent GnRH receptor antagonists. Bioorganic & Medicinal Chemistry Letters. 2002;12(16):2185-7. Available from: doi.org/10.1016/s0960-894x(02)00371-2
13. Zheng Y, Tian J, Yang W, Chen S, Liu D, Fang H, Zhang H, Ye X. Inhibition mechanism of ferulic acid against α-amylase and α-glucosidase. Food Chemistry. 2020;317:126346. Available from: doi.org/10.1016/j.foodchem.2020.126346
14. Peng X, Liu K, Hu X, Gong D, Zhang G. Hesperetin-Cu(II) complex as potential α-amylase and α-glucosidase inhibitor: Inhibition mechanism and molecular docking. Spectrochimica Acta Part A Molecular and Biomolecular Spectroscopy. 2023;290:122301. . Available from: doi.org/10.1016/j.saa.2022.122301
15. Almehmadi M, Alsaiari AA, Allahyani M, Alsharif A, Aljuaid A, Saha S, Asif M. Computational Studies and Antimicrobial Activity of 1-(benzo[d]oxazol-2-yl)-3,5-Diphenylformazan Derivatives. Current Computer Aided Drug Design. 2024;20(6): 835-846. Available from: doi.org/10.2174/1573409919666230703103135.
16. Kayes MR, Saha S, Alanazi MM, Ozeki Y, Pal D, Hadda TB, Legssyer A, Kawsar SMA. Macromolecules: Synthesis, antimicrobial, POM analysis and computational approaches of some glucoside derivatives bearing acyl moieties. Saudi Pharmaceutical Journal. 2023;31(11):101804. Available from: doi.org/10.1016/j.jsps.2023.101804
17. Kawsar SMA, Munia NS, Saha S, Ozeki Y. In Silico Pharmacokinetics, Molecular Docking and Molecular Dynamics Simulation Studies of Nucleoside Analogs for Drug Discovery-A Mini Review. Mini Reviews in Medicinal Chemistry. 2023. Available from: doi.org/10.2174/0113895575258033231024073521.
18. Saha S, Prinsa, Jakhmola V, Mahato AK, Srivastava S, Dobhal K, Kawsar SMA. In Silico Assessment of the Role of Iridoid in the Treatment of Zika and Influenza Virus Infection. Philippine Journal of Science. 2023; 152(5): 1953-1988. Available from: doi.org/10.56899/152.05.35
19. Gnana RPM, Devhare LD, Dharmamoorthy G, Khairnar MV, Prasidha R. Synthesis, Characterisation, Molecular Docking Studies and Biological Evaluation of Novel Benzothiazole Derivatives as EGFR Inhibitors for Anti-breast Cancer Agents. International Journal of Pharmaceutical Quality Assurance. 2023; 14(3):475-480. Available from: doi.org/10.25258/ijpqa.14.3.03
20. Khalaf KA, Omar AO. Synthesis, Pharmacological Evaluation, and Docking Studies of Ethyl Coumarilate Derivatives as Potential Anti-bladder Cancer in a Mouse Model. International Journal of Drug Delivery Technology. 2023; 13(4): 1548-1556. Available from: doi.org/10.25258/ijddt.13.4.66
21. Modekar SD, Mohale DS, Kochar NI, Chandewar AV. Box-Behnken Design for Formulation, Characterization and In-vivo Antidiabetic Activity of Pioglitazone Loaded Nanostructured Lipid Carriers. International Journal of Drug Delivery Technology. 2023; 13(4): 1465-1470. Available from: doi.org/10.25258/ijddt.13.4.53